

Materials. All reagents were of analytical grade and used as received without further purification. The chemicals including $ZrCl_4$, mercaptoacetic acid (MA), and $Cu(NO_3)_2 \cdot 2.5(H_2O)$ were purchased from Sigma-Aldrich. Mercaptosuccinic acid (MSA), formic acid (FA), and ethanol were purchased from Merk. $Cd(NO_3)_2 \cdot 4(H_2O)$ from Acros Organics, $Pb(NO_3)_2$, $Fe(NO_3)_3 \cdot 9(H_2O)$, $Zn(NO_3)_2 \cdot 6(H_2O)$ $Co(NO_3)_2 \cdot 6H_2O$, $Ni(NO_3)_2 \cdot 6(H_2O)$ from Fisher Scientific, UK. Deionized water (DI) was used to prepare the solutions (MilliQ).

Characterization. Fourier transform Infrared (FTIR) spectroscopy was conducted on ThermoScientific iS-10. Scanning, electron microscopy (SEM) was conducted on Thermofisher (USA) Quattro S Field Emission Gun, Environmental SEM (FEGSEM). X-ray diffraction (XRD) patterns were acquired on a Bruker powder diffractometer equipped with $Cu K\alpha$ radiation (35kV, 15mA) at a scan rate of $10^\circ \text{ min}^{-1}$ with step width 0.015° and Scan range $5 \sim 80^\circ$. Inductively coupled plasma mass spectrometer (ICP-MS) was employed to determine the content of various elements in aqueous solutions.

Synthesis of Zr-MSA. In a clean, dry scintillation vial, $ZrCl_4$ (150 mg, 0.64 mmol), MSA (100 mg, 0.66 mmol), and 100 μL of formic acid, used as the modulator in this reaction, (FA, 4eq. relative to $ZrCl_4$) were combined in 2 mL of DI water and sonicated for 10 minutes. Then, the mixture was kept in thermal block at 80°C . After 2 hours, the reaction mixture was cooled down to room temperature, and the white precipitate was collected by centrifugation, followed by washing with 10mL of DI water (twice) then 10mL of ethanol (three times). Finally, the solid was dried under vacuum at 60°C overnight. (**Yield=160mg**).

Synthesis of Zr-MSA-MA.

In a clean, dry scintillation vial, $ZrCl_4$ (125 mg, 0.53 mmol), MSA (80 mg, 0.53 mmol), 50 μL of MA, and 50 μL of FA, used as the modulator in this reaction, were combined in 2mL of DI water and sonicated for 10 minutes. Then, the mixture was kept in thermal block at 80°C . After 2 hours, the reaction mixture was cooled down to room temperature, and the white precipitate was collected by centrifugation, followed by washing with 10 mL of DI water (twice) then 10 mL of ethanol (three times). Finally, the solid was dried under vacuum at 60°C overnight. (**Yield=130 mg**).

Kinetics Studies.

Cadmium. In eight sealed glass vials, 10.5mg of Zr-MSA-MA was left to stir at room temperature with 20 mL of 200 ppm $Cd(II)$ for specific time intervals (0.5, 1, 1.5, 2, 3, 4, 5, and 6 hours). After each time interval, the supernatant was collected from each vial separately by centrifugation at 6000 rpm for 10minutes, followed by microfiltration membrane (pore size, $0.22 \mu\text{m}$). The $Cd(II)$ concentration in the supernatant was then measured using an inductively coupled plasma mass spectrometer (ICP-MS).

Lead. In eight sealed glass vials, 10.5 mg of Zr-MSA-MA was left to stir at room temperature with 20 mL of 200 ppm Pb(II) for different time intervals (0.5, 1, 1.5, 2, 3, 4, 5, and 6 hours). After each time interval, the supernatant was collected from each vial separately by centrifugation at 6000 rpm for 10 minutes, followed by microfiltration membrane (pore size, 0.22 μm). The Pb(II) concentration in the supernatant was then measured using an inductively coupled plasma mass spectrometer (ICP-MS).

Dose-dependency Studies.

Cadmium. In five sealed glass vials, different weights of Zr-MSA-MA (5, 10, 20, 30 and 40 mg) was left to stir at room temperature with 20 mL of 200 ppm Cd(II) for 4h. After which, the supernatant was collected from each vial separately by centrifugation at 6000 rpm for 10 minutes, followed by microfiltration membrane (pore size, 0.22 μm). The Cd(II) concentration in the supernatant was then measured using an inductively coupled plasma mass spectrometer (ICP-MS).

Lead. In five sealed glass vials, different weights of Zr-MSA-MA (5, 10, 20, 30 and 40 mg) was left to stir at room temperature with 20 mL of 200 ppm Pb(II) for 4h. After which, the supernatant was collected from each vial separately by centrifugation at 6000 rpm for 10 minutes, followed by microfiltration membrane (pore size, 0.22 μm). The Pb(II) concentration in the supernatant was then measured using an inductively coupled plasma mass spectrometer (ICP-MS).

pH-dependency Studies.

Cadmium. In five sealed glass vials, 10.5 mg of Zr-MSA-MA was left to stir at 450 rpm at room temperature with 20 mL of 200 ppm Cd(II) of different pH (2, 4, 5, 6, and 8). After 4h, the supernatant was collected from each vial separately by centrifugation at 6000 rpm for 10 minutes, followed by microfiltration membrane (pore size, 0.22 μm). The Cd(II) concentration in the supernatant was then measured using an inductively coupled plasma mass spectrometer (ICP-MS).

Lead. In five sealed glass vials, 10.5 mg of Zr-MSA-MA was left to stir at 450 rpm at room temperature with 20 mL of 200 ppm Pb(II) of different pH (2, 4, 5, 6, and 8). After 4h, the supernatant was collected from each vial separately by centrifugation at 6000 rpm for 10 minutes, followed by microfiltration membrane (pore size, 0.22 μm). The Pb(II) concentration in the supernatant was then measured using an inductively coupled plasma mass spectrometer (ICP-MS).

The desired pH of each stock solution was adjusted through the addition of either 0.1M HCl or NaOH.

Adsorption Isotherm Studies.

Cadmium. In sealed glass vials, eight separate samples of 10.5 mg Zr-MSA-MA was added into 20 mL of Cd(II) solutions of different concentrations (25, 50, 100, 200, 400, 600, 800, 1000 ppm) and stirred at 450 rpm (pH=6). After 4h, the supernatant from each vial was separately collected by centrifugation at 6000 rpm for 10 minutes, followed by microfiltration membrane (pore size,

0.22 μm). The Cd(II) concentration in the supernatant was then measured using an inductively coupled plasma mass spectrometer (ICP-MS).

Lead. In sealed glass vials, eight separate samples of 10.5 mg Zr-MSA-MA was added into 20 mL of Pb(II) solutions of different concentrations (25, 50, 100, 200, 400, 600, 800, 1000 ppm) and stirred at 450 rpm (pH=6). After 4h, the supernatant was collected from each vial separately by centrifugation at 6000 rpm for 10 minutes, followed by microfiltration membrane (pore size, 0.22 μm). The Pb(II) concentration in the supernatant was then measured using an inductively coupled plasma mass spectrometer (ICP-MS).

Regeneration Studies.

Cadmium. To probe the regeneration ability of Zr-MSA-MA MOF, a 0.45 μm nylon syringe filter was loaded with 30 mg of Zr-MSA-MA after being suspended in 10 mL of DI water. Then, 20 mL of 15 ppm of Cd(II) solution was passed through the loaded syringe filter, and the filtrate was collected for ICP analysis. The syringe filter was then washed with 1M HCl (20mL) followed by 20 mL of DI water. The Cd²⁺ uptake and washing were repeated for 10 cycles.

Lead. To probe the regeneration ability of Zr-MSA-MA MOF, a 0.45 μm nylon syringe filter was loaded with 30 mg of Zr-MSA-MA after being suspended in 10 mL of DI water. Then, 20 mL of 15 ppm of Pb(II) solution was passed through the loaded syringe filter, and the filtrate was collected for ICP analysis. The syringe filter was then washed with 1M HCl (20 mL) followed by 20 mL of DI water. The Pb(II) uptake and washing were repeated for 10 cycles.

Selectivity Studies.

The effect of competing ions on the uptake efficiency was investigated using a batch-ion exchange protocol in which 40 mg of Zr-MSA-MA was immersed in mixture made by mixing 5 mL of 25 ppm from each of the following metal ions: Pb(II), Cd(II), Cu(II), Zn(II), Mn(II), Fe(III), Co(II), and Ni(II) with stirring. After 4h, the supernatants were collected by centrifugation followed by microfiltration for determining the concentration of each ion using an inductively coupled plasma mass spectrometer (ICP-MS). The same procedure was repeated but utilizing 100 ppm of each metal ion to test the selectivity in more demanding environment.

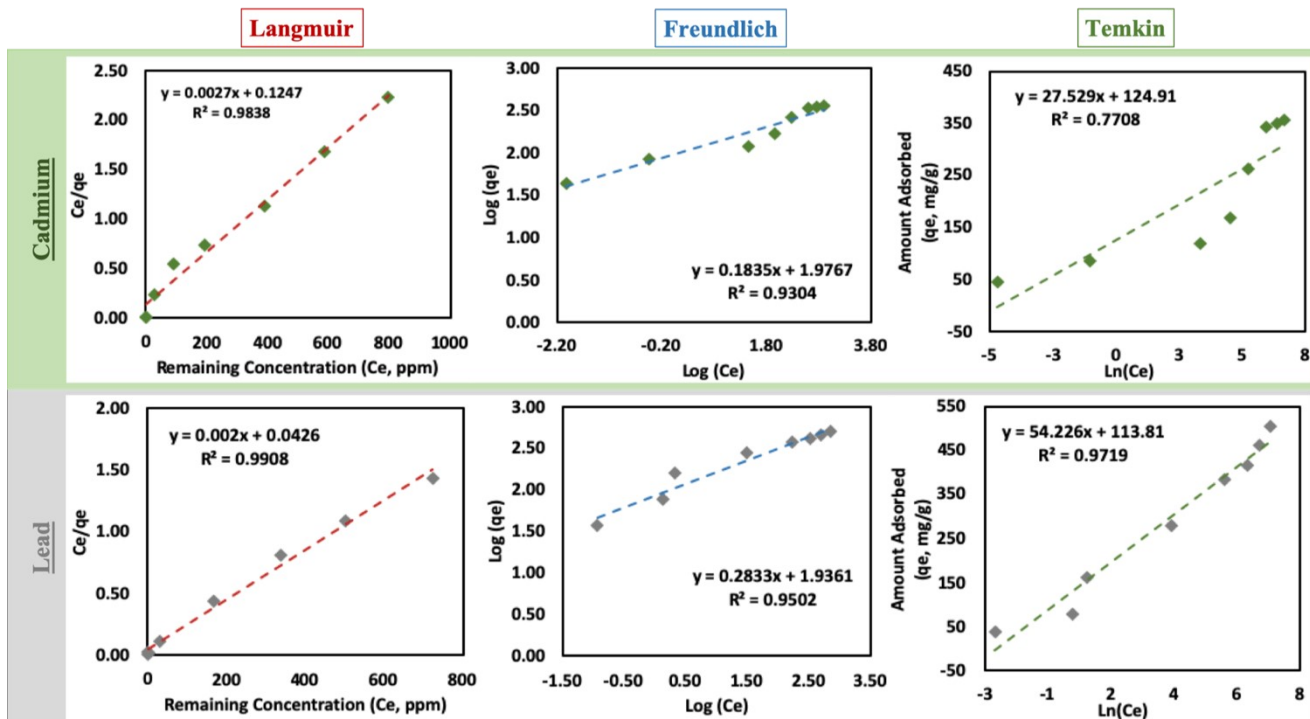


Figure S1. Investigation of Zr-MSA-MA MOF uptake behavior toward different contaminants Cd(II), Pb(II). Linear adsorption isotherms plots fitted by the (a) Langmuir, (b) Freundlich, and (c) Temkin models.

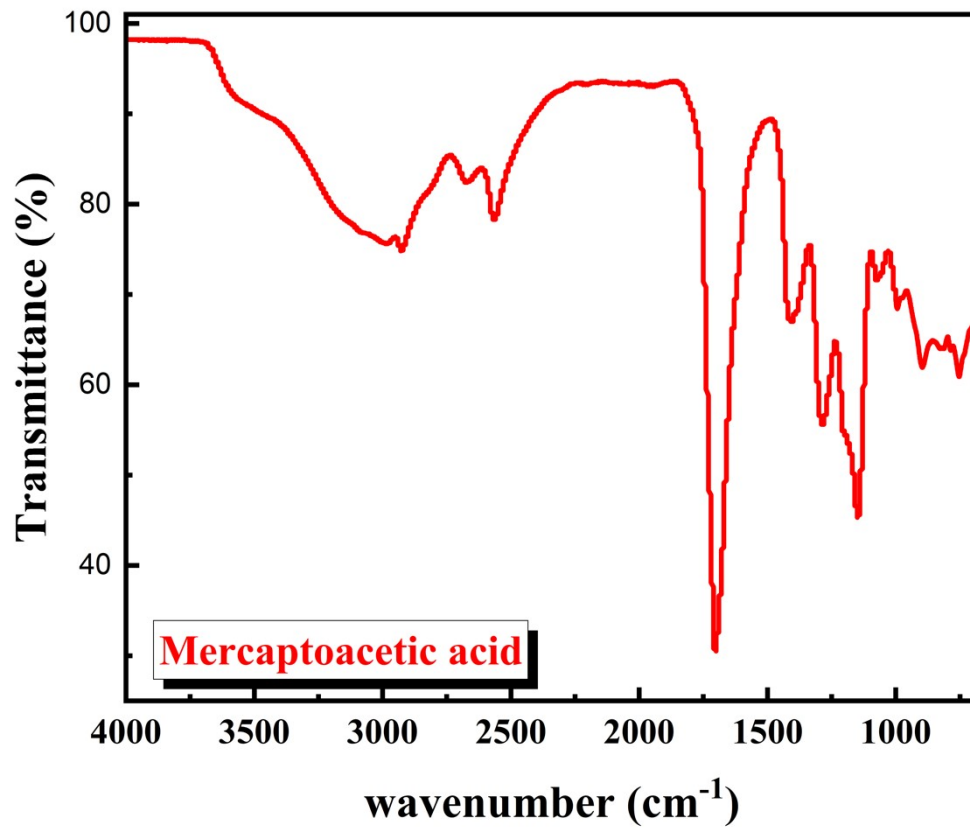


Figure S2. FTIR spectrum of the mercaptoacetic acid.

Table S1. Adsorption Isotherm Fitting Parameters of the Langmuir, Freundlich, and Temkin Models for the Three Contaminants.

Model	Cd(II)	Pb(II)
<u>Langmuir</u>		
slope	0.0027	0.0020
q_m	370.37	500.00
Uptake mmol/g	3.29	2.41
intercept	0.1247	0.0426
b	0.0217	0.0469
R²	0.9838	0.9908
<u>Freundlich</u>		
slope	0.1835	0.2833
n	5.4496	3.5298
intercept	1.9767	1.9361
K_f	94.776	86.318
R²	0.9304	0.9502
<u>Temkin</u>		
Slope	27.529	54.226
b	90.04	45.71
Intercept	124.91	113.81
K_T	93.447	8.156
R²	0.7708	0.9719

Table S2. Maximum Adsorption capacities (mg/g) for Pb(II), Cd(II), and Cr(VI) species by MOF-based sorbents.

	Adsorbent	Capacity (mg/g)	Ref.
	Zr-MSA-MA	500.00	This Work
Pb(II)	Zn(ADB)L0.5]·1.5DMF	463.52	[1]
	TIF-A1/ chitosan	397.3	[2]
	AMCA-MIL-53(Al)	390	[3]
	UiO-66-ATA	387	[4]
	ED-MIL-100(Fe)	378.8	[5]
	MOF/Gum carrageenan composite (MGC)	374.7	[6]
	UiO-66-EDTA	357.9	[7]
	ZnO/ZnFe ₂ O ₄ /C	344.83	[8]
	MOF-808-EDTA(BS-HMT)	313	[9]
	MIL-125-HQ	262.1	[10]
	Zinc (II) metal–organic framework (TMU-5)	251	[11]
	Fe–Mg MOF	196	[12]
	SS-NH ₂ -UiO-66-5	186.14	[13]
	UiO-66-NH ₂	177.35	[14]
	MIL-100(Fe)-DE hybrid material	155	[15]
	CS-ZIF-8 composite	131.14	[16]
	DUT-67	98.5	[17]
Cd(II)	MOF-808-EDTA(BS-HMT)	528.00	[1]
	LDH/MOF	415.30	[2]
	Zr-MSA-MA	370.37	This Work
	FJI-H9	286	[3]
	MOF-808@PAN	225	[4]
	UiO-66-EDA	217.39	[5]
	MOF@CSC composite sponge	193.35	[6]
	Fe–Mg MOF	191	[7]
	UiO-66-NH ₂	177.35	[8]
	Fe ₃ O ₄ @MOF-235(Fe)-OSO ₃ H	163.9	[9]
	Modified UiO-66 with melamine (MUiO-66)	146.6	[10]
	MIL-125-HQ	103	[11]
	UiO-66-SH	77.42	[12]
	Zr-DMBD	43.8	[13]

References for Pb sorbents

- [1] Yu, C.-X., et al. (2020). "Highly Efficient and Facile Removal of Pb²⁺ from Water by Using a Negatively Charged Azoxy-Functionalized Metal–Organic Framework." *Crystal Growth & Design* **20**(8): 5251-5260.
- [2] Ma, Y., et al. (2022). "Confined growth of MOF in chitosan matrix for removal of trace Pb(II) from reclaimed water." *Separation and Purification Technology* **294**.
- [3] Alqadami, A. A., et al. (2018). "Development of citric anhydride anchored mesoporous MOF through post synthesis modification to sequester potentially toxic lead (II) from water." *Microporous and Mesoporous Materials* **261**: 198-206.
- [4] Xiong, C., et al. (2020). "Efficient Selective Removal of Pb (II) by Using 6-Aminothiouracil-Modified Zr-Based Organic Frameworks: From Experiments to Mechanisms." *ACS Appl Mater Interfaces* **12**(6): 7162-7178.
- [5] Zhang, H., et al. (2019). "Influence of fulvic acid on Pb (II) removal from water using a post-synthetically modified MIL-100(Fe)." *J Colloid Interface Sci* **551**: 155-163.
- [6] Ahmed, G. H. G., et al. (2024). "High-performance copper terephthalic acid metal-organic framework/gum Arabic/carrageenan composite beads for efficient lead (II) removal from aqueous solutions." *Int J Biol Macromol* **282**(Pt 6): 137448.
- [7] Wu, J., et al. (2019). "Efficient removal of metal contaminants by EDTA modified MOF from aqueous solutions." *J Colloid Interface Sci* **555**: 403-412.
- [8] Chen, D., et al. (2016). "Ion exchange induced removal of Pb(ii) by MOF-derived magnetic inorganic sorbents." *Nanoscale* **8**(13): 7172-7179.
- [9] Peng, Y., et al. (2018). "A versatile MOF-based trap for heavy metal ion capture and dispersion." *Nat Commun* **9**(1): 187.
- [10] Abdelhameed, R. M., et al. (2019). "Post-synthetic modification of MIL-125 with bis-quinoline Mannich bases for removal of heavy metals from wastewater." *Microporous and Mesoporous Materials* **279**: 26-36.
- [11] Tahmasebi, E., et al. (2015). "Application of mechanosynthesized azine-decorated zinc (II) metal-organic frameworks for highly efficient removal and extraction of some heavy-metal ions from aqueous samples: a comparative study." *Inorg Chem* **54**(2): 425-433.
- [12] Abo El-Yazeed, W. S., et al. (2020). "Facile fabrication of bimetallic Fe-Mg MOF for the synthesis of xanthenes and removal of heavy metal ions." *RSC Adv* **10**(16): 9693-9703.
- [13] Li, Y.-H., et al. (2022). "Seignette salt induced defects in Zr-MOFs for boosted Pb(II) adsorption: universal strategy and mechanism insight." *Chemical Engineering Journal* **442**.
- [14] Wang, K., et al. (2017). "Efficient Removal of Pb (II) and Cd (II) Using NH₂-Functionalized Zr-MOFs via Rapid Microwave-Promoted Synthesis." *Industrial & Engineering Chemistry Research* **56**(7): 1880-1887.
- [15] Uthappa, U. T., et al. (2020). "Engineering MIL-100(Fe) on 3D porous natural diatoms as a versatile high performing platform for controlled isoniazid drug release, Fenton's catalysis for malachite green dye degradation and environmental adsorbents for Pb²⁺ removal and dyes." *Applied Surface Science* **528**.
- [16] Wang, C., et al. (2022). "Efficient removal of Cu(II) and Pb(II) from water by in situ synthesis of CS-ZIF-8 composite beads." *Journal of Environmental Chemical Engineering* **10**(3). [18] Geisse, A. R., et al. (2019). "Removal of lead ions from water using thiophene-functionalized metal-organic frameworks." *Chem Commun (Camb)* **56**(2): 237-240.

References of Cd sorbents

- [1] Peng, Y., et al. (2018). "A versatile MOF-based trap for heavy metal ion capture and dispersion." *Nat Commun* **9**(1): 187.
- [2] Soltani, R., et al. (2021). "A novel and facile green synthesis method to prepare LDH/MOF nanocomposite for removal of Cd (II) and Pb (II)." *Sci Rep* **11**(1): 1609.
- [3] Xue, H., et al. (2016). "A regenerative metal-organic framework for reversible uptake of Cd(ii): from effective adsorption to in situ detection." *Chem Sci* **7**(9): 5983-5988.
- [4] Efome, J. E., et al. (2018). "Insight Studies on Metal-Organic Framework Nanofibrous Membrane Adsorption and Activation for Heavy Metal Ions Removal from Aqueous Solution." *ACS Appl Mater Interfaces* **10**(22): 18619-18629.
- [5] Ahmadijokani, F., et al. (2021). "Ethylenediamine-functionalized Zr-based MOF for efficient removal of heavy metal ions from water." *Chemosphere* **264**(Pt 2): 128466.
- [6] Nassef, H. M., et al. (2024). "Synthesis and characterization of new composite sponge combining of metal-organic framework and chitosan for the elimination of Pb (II), Cu (II) and Cd (II) ions from aqueous solutions: Batch adsorption and optimization using Box-Behnken design." *Journal of Molecular Liquids* **394**.
- [7] Abo El-Yazeed, W. S., et al. (2020). "Facile fabrication of bimetallic Fe-Mg MOF for the synthesis of xanthenes and removal of heavy metal ions." *RSC Adv* **10**(16): 9693-9703.
- [8] Wang, K., et al. (2017). "Efficient Removal of Pb (II) and Cd (II) Using NH₂-Functionalized Zr-MOFs via Rapid Microwave-Promoted Synthesis." *Industrial & Engineering Chemistry Research* **56**(7): 1880-1887.
- [9] Moradi, S. E., et al. (2016). "Sulfonated metal organic framework loaded on iron oxide nanoparticles as a new sorbent for the magnetic solid phase extraction of cadmium from environmental water samples." *Analytical Methods* **8**(33): 6337-6346.
- [10] Abdelmoaty, A. S., et al. (2022). "High Performance of UiO-66 Metal–Organic Framework Modified with Melamine for Uptaking of Lead and Cadmium from Aqueous Solutions." *Journal of Inorganic and Organometallic Polymers and Materials* **32**(7): 2557-2567.
- [11] Abdelhameed, R. M., et al. (2019). "Post-synthetic modification of MIL-125 with bis-quinoline Mannich bases for removal of heavy metals from wastewater." *Microporous and Mesoporous Materials* **279**: 26-36.
- [12] Chen, X., et al. (2024). "New insight into the co-removal of arsenic and cadmium from wastewater by using thiol-functionalized UiO-66: A mechanistic study and real water test." *Separation and Purification Technology* **332**.
- [13] Ding, L., et al. (2018). "Thiol-Functionalized Zr-Based Metal–Organic Framework for Capture of Hg (II) through a Proton Exchange Reaction." *ACS Sustainable Chemistry & Engineering* **6**(7): 8494-8502.